

Two-Step Glass Transition Induced by Attractive Interactions in Quasi-Two-Dimensional Suspensions of Ellipsoidal Particles

Chandan K. Mishra,^{1,*} Amritha Rangarajan,¹ and Rajesh Ganapathy^{2,†}

¹*Chemistry and Physics of Materials Unit, Jawaharlal Nehru Centre for Advanced Scientific Research, Jakkur, Bangalore 560064, India*

²*International Centre for Materials Science, Jawaharlal Nehru Centre for Advanced Scientific Research, Jakkur, Bangalore 560064, India*

(Received 28 November 2012; published 29 April 2013)

We study experimentally the glass transition dynamics in quasi-two-dimensional suspensions of colloidal ellipsoids, aspect ratio $\alpha = 2.1$, with repulsive as well as attractive interactions. For the purely repulsive case, we find that the orientational and translational glass transitions occur at the same area fraction. Strikingly, for intermediate depletion attraction strengths, we find that the orientational glass transition precedes the translational one. By quantifying structure and dynamics, we show that quasi-long-range ordering is promoted at these attraction strengths, which subsequently results in a two-step glass transition. Most interestingly, within experimental certainty, we observe reentrant glass dynamics only in the translational degrees of freedom.

DOI: [10.1103/PhysRevLett.110.188301](https://doi.org/10.1103/PhysRevLett.110.188301)

PACS numbers: 82.70.Dd, 64.70.pv

The microscopic underpinnings of glasses and the glass transition continue to remain one of the grand challenges in condensed matter physics [1]. There have been significant advances in our understanding of the glassy state and the approach to this state using model systems of colloids with isotropic shape and/or interactions [2–6]. Although particle shape strongly influences their packing [7], it is only recently that experiments have probed its role in glass transition phenomena [8,9]. In particular, quasi-two-dimensional (2D) experiments on prolate colloidal ellipsoids of intermediate aspect ratio $\alpha = 6$ and with purely repulsive interactions show two glass transitions [9]. The first corresponds to the orientational freezing of particle dynamics and the second to their translational freezing and is in qualitative agreement with experiments on liquid crystals [10], molecular mode coupling theory (MMCT) predictions, and computer simulations [11,12]. Nevertheless, even in 2D, experiments are yet to confirm that ellipsoids with $\alpha < 2.5$ show a single glass transition as predicted by MMCT [13]. Apart from the rich phase behavior resulting from particle shape anisotropy, recent colloid experiments have shown that interaction anisotropy can result in novel phases [14]. Interaction anisotropy is likely to have wider relevance in the dynamics of gels and glasses also [8,15]. It is well established that even with isotropic short-range attraction, hard spheres show rich reentrant glass phenomena [5,16]. At a fixed volume fraction greater than the repulsive glass transition volume fraction, a repulsive glass (RG) melts to an ergodic fluid and forms a novel glass—attractive glass (AG)—at even higher interaction strengths [5,16]. However, the consequences of interaction anisotropy for reentrant glass behavior are yet to be explored by theory, simulations and experiments.

In this Letter, we demonstrate experimentally the key role of particle shape and interaction anisotropy in reentrant glass phenomena. Our system is comprised of colloidal ellipsoids, $\alpha = 2.1$, interacting via a short-range depletion interaction. Since the strength of the depletion interaction between particles also depends on their local curvature [17], for ellipsoidal particles this leads to an anisotropic attractive interaction. Using a combination of mode coupling theory (MCT) scaling arguments and the size distribution and scaling of most-mobile particle clusters, we first show that, without attraction, the orientational and translational glass transitions, ϕ_g^R and ϕ_g^T respectively, occur at the same area fraction ϕ . (Fig. 1). Remarkably, onset of quasi-long-range ordering at intermediate attraction strengths results in a two-step glass transition with an intervening orientational glass regime (Figs. 2–4).

Colloidal ellipsoids were synthesized using well-established protocols [18]. The major and minor axes were $2l = 2.1 \mu\text{m}$ and $2w = 1 \mu\text{m}$ with polydispersities of 11% and 8%, respectively. We used sodium carboxyl methyl cellulose (NaCMC, Fischer-Scientific, mol. wt. 700 000, $r_g \approx 60 \text{ nm}$) as the depletant. Suspensions of ellipsoids in water, at suitable depletant concentration c_p , below the overlap concentration $c^* = 0.11 \text{ mg/ml}$, were loaded in wedge-shaped cells and left standing under gravity to allow sedimentation to the 2D regions of the cell (see the Supplemental Material [19]). For each c_p , experiments were done for at least six ϕ 's ranging from $0.23 < \phi < 0.84$ [9]. Video microscopy was done using a 100X oil immersion objective (Leica, Plan-Apochromat, numerical aperture 1.4) at a frame rate of 5 frames per second for a typical duration of 20 minutes. The center-of-mass coordinates and the orientations of the ellipsoids were

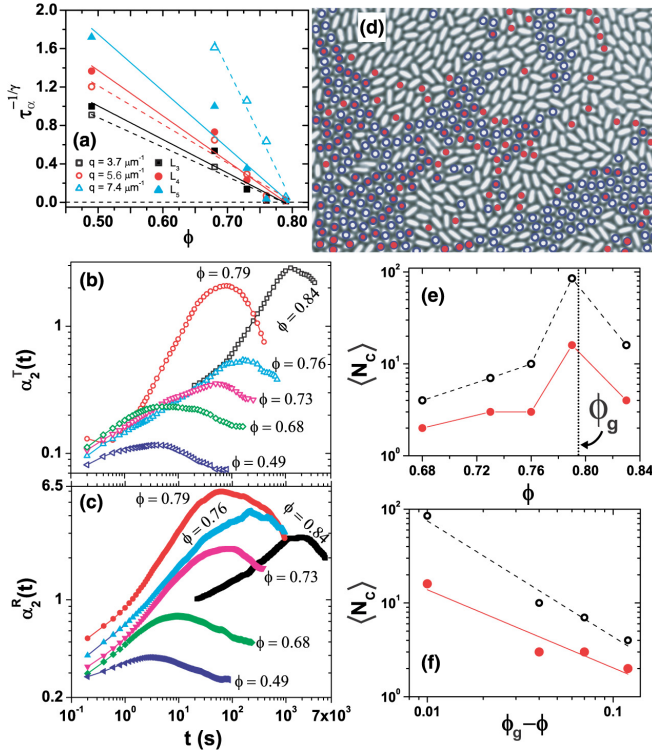


FIG. 1 (color online). Solid and open symbols in all subplots correspond to orientational and translational DOF, respectively. (a) $\tau_\alpha^{-1/\gamma}$ vs ϕ . Here, $\gamma^T = 1.93$ and $\gamma^R = 2.24$. (b) Translational non-Gaussian parameter $\alpha_2^T(t)$. (c) Orientational non-Gaussian parameter $\alpha_2^R(t)$ at various ϕ 's. (d) Top 10% translationally most-mobile (open blue circles) and orientationally most-mobile (solid red circles) particles at $\phi = 0.79$. (e) $\langle N_c \rangle$ at different ϕ 's. (f) $\langle N_c \rangle$ vs $(\phi_g - \phi)$. Lines in (a) and (f) are linear and power law fits to the data, respectively.

obtained using IMAGEJ and the data were analyzed using standard MATLAB algorithms [20]. The spatial resolution was found to be 60 nm and the angular resolution was 1° .

We first determined ϕ_g^R and ϕ_g^T for ellipsoids with purely repulsive interactions (see the Supplemental Material, movie 1 [19]). Unlike observations on ellipsoids with $\alpha = 6$ [9], in our experiments, even after months, we did not observe the formation of pseudonematic domains even at the highest $\phi = 0.84$ studied. Following Refs. [9,21], we obtained the translational and orientational relaxation times, τ_α , with ϕ , from the long-time decay of the self-intermediate scattering function, $F_s(\mathbf{q}, t) = \frac{1}{N} \langle \sum_{j=1}^N e^{i\mathbf{q} \cdot (\mathbf{r}_j(t+t_0) - \mathbf{r}_j(t))} \rangle$ and the n th order dynamic orientational correlation function, $L_n(t) = \frac{1}{N} \langle \sum_{j=1}^N \cos n(\theta_j(t+t_0) - \theta_j(t)) \rangle$, respectively [9]. Here, N is the total number of particles, $\mathbf{r}_j(t)$ and $\theta_j(t)$ are the position and orientation of the j th ellipsoid at time t , t_0 is the lag time, \mathbf{q} is the wave vector and the $\langle \rangle$ denotes time averaging. Although at low ϕ , $F_s(\mathbf{q}, t)$ and $L_n(t)$ decay exponentially, at high ϕ , both show a two-step relaxation that is typical of glass-forming liquids [12,19,22]. The first

step corresponds to rattling of particles in cages formed by their neighbors, the β relaxation, and the second to cage rearrangements and the subsequent escape of particles, the α relaxation [22].

The onset of caging was evidenced by nonexponential relaxation in $F_s(q, t)$ and $L_n(t)$ for $\phi = 0.73$ (see the Supplemental Material [19]). While at $\phi = 0.79$, $F_s(q, t)$ decayed completely and $L_n(t)$ by $\approx 25\%$ over 700 s, for $\phi = 0.84$, $F_s(q, t)$ decayed by only about 20% and $L_n(t)$ by $\approx 7\%$ over 4000 s (see the Supplemental Material [19]). This suggests an ergodic-nonergodic transition with $0.79 < \phi_g^{R,T} < 0.84$ (see the Supplemental Material [19]). We determined ϕ_g from MCT scaling analysis. As per MCT, as ϕ_g is approached, τ_α diverges as $\tau_\alpha(\phi) \propto (\phi_g - \phi)^{-\gamma}$ where $\gamma = \frac{1}{2a} + \frac{1}{2b}$ [22]. Here a and b are exponents in the critical decay law $F_s(q, t) = f_q + h_q t^{-a}$ and the von Schweidler law $F_s(q, t) = f_q - h_q t^b$, respectively [9,12]. f_q and h_q are the plateau height and amplitude. In our experiments we obtained b from fits to $F_s(q, t)$ and $L_n(t)$. Owing to poor temporal resolution in the early β regime, we obtained a from Ref. [22]. Consistent with MCT predictions, we find that $\tau_\alpha^{-1/\gamma}$ is linear in ϕ (Fig. 1(a)) for all q 's and n 's studied. Strikingly, this scaling yields the same $\phi_g = 0.80 \pm 0.01$ for both translational and orientational degrees of freedom (DOF). We have also determined the ideal glass transition area fraction ϕ_0 , where diffusive dynamics cease, using the Vogel-Tammann-Fulcher model, $\phi_0 = 0.89 \pm 0.02$ (see the Supplemental Material [19]). $\phi_0 > \phi_g$ and is in the vicinity of the predicted value ($\phi_0 \approx 0.88$) for bidisperse ellipsoids, $\alpha \approx 2.2$, in 2D [23].

To show that ϕ_g is indeed at 0.80 ± 0.01 , we have quantified the size distribution and scaling of the most-mobile particle clusters. These clusters, believed to be pathways for structural relaxation in supercooled liquids and glasses [24], show qualitative trends with ϕ across ϕ_g [4,9]. To quantify these, we first determined deviations from Gaussian dynamics using the non-Gaussian parameter $\alpha_2(t) = \frac{\langle \Delta r(t)^4 \rangle}{2(\langle \Delta r(t)^2 \rangle)^2} - 1$ [4], which peaks in the vicinity of the cage rearrangement time t^* . Here $\Delta r(t)$ is the particle displacement over time t . The coupling between rotational and translational DOF can lead to non-Gaussian effects in the lab frame for ellipsoids even in the dilute limit [25]. We have verified that all trends reported here are preserved in the body frame of ellipsoids as well, where this coupling is absent. Both t^* and the peak amplitude $\alpha_2^{T,R}(t=t^*)$ increase on approaching ϕ_g [Figs. 1(b) and 1(c)]. In the vicinity of ϕ_g and beyond, absence of large cooperative cage rearrangements can lead to a decrease in t^* (see Refs. [4,9] and the Supplemental Material [19]) and is consistent with our observations of $t_{\phi=0.79}^* < t_{\phi=0.76}^*$. Since $\alpha_2(t)$ is fairly sensitive to noise, the increase in t^* at $\phi = 0.84$ is

probably due to particle tracking errors from negligible particle displacement that are comparable to the spatial resolution in our experiments [19,26]. The top 10% most-mobile particles over t^* are found to be spatially clustered [Fig. 1(d)]. Two most-mobile particles belong to the same cluster if one ellipsoid, when expanded 1.4 times and maintaining its orientation, encompasses the other's center, subject to the condition that there is no immobile ellipsoid between them. We find that a significant fraction of orientationally most-mobile particles are also translationally most-mobile and is consistent with the absence of pseudonematic domains [Fig. 1(d)]. Analogous to observations on 3D colloidal glasses of hard spheres [4], the weighted mean cluster size [27] $\langle N_c^{T,R} \rangle = \sum_n n^2 P(n) / \sum_n n P(n)$ increases on approaching ϕ_g and shows a sharp decrease beyond ϕ_g [Fig. 1(e)]. These observations confirm that $0.79 < \phi_g^T, \phi_g^R < 0.84$ and is consistent with $\phi_g = 0.80 \pm 0.01$ [Fig. 1(a)]. As observed in Refs. [9,28], $\langle N_c^{T,R} \rangle \propto (\phi_g - \phi)^{-\eta}$ [Fig. 1(f)].

Before we move on to colloidal ellipsoids with short-range attraction, a little background on their spherical counterparts will be useful here. For hard spheres with short range depletion attraction ($\frac{r_g}{r} < 0.15$) [29], MCT predicted the existence of an attractive glassy phase at high attraction strengths and for densities $\Phi_g < \Phi < \Phi_{A_3}$ [29]. Here, Φ_{A_3} is the density beyond which the distinction between the repulsive and attractive glass vanishes. This prediction was confirmed via dynamic light scattering experiments on colloid-polymer mixtures which showed reentrant behavior in $F_s(q, t)$ [5]. For a narrow range of Φ 's with $\Phi > \Phi_g$, and at low and high attraction strengths, $F_s(q, t)$ showed a two-step relaxation and only a partial decay even at long times. Whereas, at intermediate attraction strengths, $F_s(q, t)$ decayed completely with a shift in Φ_g to higher Φ 's. Though the short-time dynamics in attractive glasses is dominated by bond breaking, recent simulations have shown that analogous to repulsive glasses structural relaxation at long times is still governed by cage rearrangements [30].

In 2D the relationship between c_p and attraction strength U is not well understood [31]. Therefore for all c_p 's investigated here, we directly measured the change in depth of the scaled depletion potential $\Delta u = -\frac{\Delta U}{k_B T}$, averaged over all orientations, with respect to $c_p = 0$, from dimer life time measurements (see the Supplemental Material [19] and Ref. [32]). Here k_B is the Boltzmann constant and T is the temperature. Figures 2(a) and 2(b), shows $F_s(q = 5.6 \mu\text{m}^{-1}, t)$ and $L_3(t)$ for $\phi \approx 0.79 \approx \phi_g$ for different Δu 's, respectively. For $\Delta u = 0$ and $\Delta u = 1.47$, both $F_s(q, t)$ and $L_3(t)$ show a two-step decay [inset to Figs. 2(a) and 2(b)]. The larger plateau value at long times for $\Delta u = 1.47$ implies a relatively stronger freezing-in of long-wavelength collective density fluctuations [5]. However, for an intermediate value $\Delta u = 1.16$, while

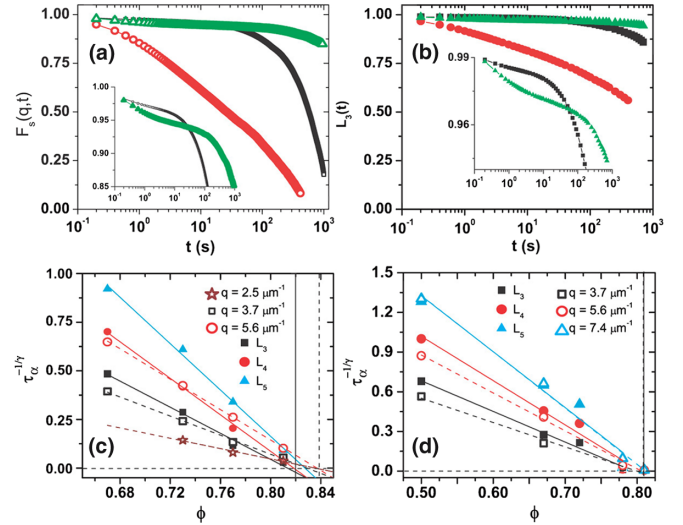


FIG. 2 (color online). (a) $F_s(q = 5.6 \mu\text{m}^{-1}, t)$ and (b) $L_3(t)$ for $\Delta u = 0$ at $\phi = 0.79$ (black squares), $\Delta u = 1.16$ at $\phi = 0.81$ (red circles), $\Delta u = 1.47$ at $\phi = 0.81$ (green triangles). Inset to (a) and (b) —with expanded y axis shows two-step relaxation. MCT scaling of τ_α for $\Delta u = 1.16$ (c) and $\Delta u = 1.47$ (d). Solid and open symbols correspond to orientational and translational scaling of τ_α , respectively. The lines are linear fits to the data. The solid and dashed vertical lines in (c) and (d) denote ϕ_g^R and ϕ_g^T , respectively.

$F_s(q, t)$ decayed completely only a partial decay was observed in $L_n(t)$ [Fig. 2(b)]. To determine if ϕ_g at intermediate attraction strength has indeed shifted to a $\phi > \text{RG}\phi_g$, we performed the aforementioned MCT scaling for all Δu 's studied here. In line with theoretical predictions [29], $\tau_\alpha^{-1/\gamma}$ is linear in ϕ for attractive glasses also and allows us to extract ϕ_g^R and ϕ_g^T [Figs. 2(c) and 2(d)]. Strikingly, for $\Delta u = 1.16$ we observe a two-step glass transition with $\phi_g^R = 0.82 \pm 0.01$ and $\phi_g^T = 0.84 \pm 0.01$ [Fig. 2(c)]. For $\Delta u = 1.47$, ϕ_g^T reverts to a lower ϕ with $\phi_g^T = 0.81 \pm 0.01$ and $\phi_g^R = 0.81 \pm 0.02$ [Fig. 2(d)] (see the Supplemental Material, movie 2 [19]).

To further validate the above observations, we explored the complete phase diagram in the $(\phi, \Delta u)$ plane with $\alpha_2^{T,R}(t = t^*)$, $F_s(q, t_\infty)$, and $L_3(t_\infty)$ as the quantifier of particle dynamics. Here t_∞ denotes experimental time duration. Figures 3(a) and 3(b) show the translational and orientational phase diagram respectively, along with MCT predicted glass transitions. Since sedimentation to the 2D regions of the cell was extremely slow for ellipsoids with attractive interactions, we were unable to collect data beyond $\phi \approx 0.81$. Overall, $\alpha_2^T(t^*) < \alpha_2^R(t^*)$, indicating that orientational relaxations are relatively more hindered compared to translational ones. While at low ϕ and at small Δu 's, an ergodic phase was observed, for large Δu 's we found percolating networks of ellipsoids which we identified as a gel phase (Supplemental Material, movie 3 [19]) [5]. Most remarkably, at a fixed $\phi \geq \text{RG}\phi_g$

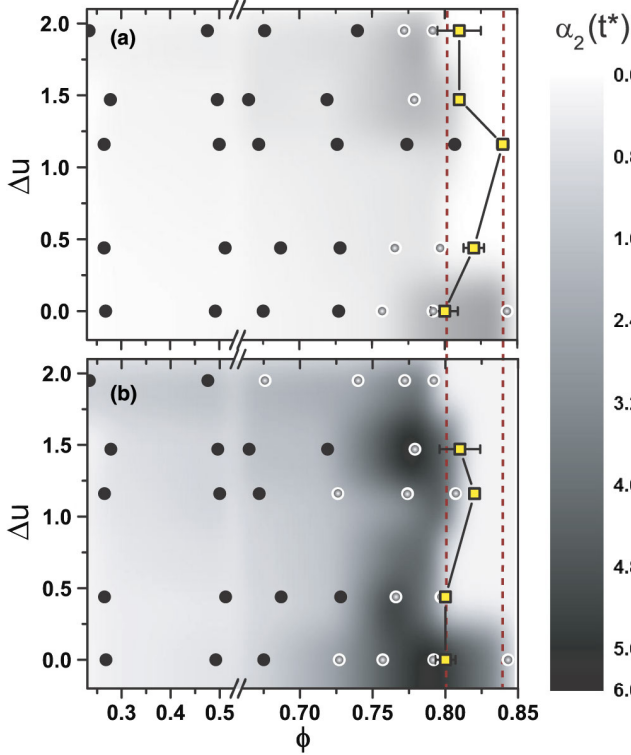


FIG. 3 (color online). Phase diagram in $(\Delta u, \phi)$ plane. The circles represent the Δu and ϕ at which experiments were performed. (a) Translational DOF. (b) Orientational DOF. The black circles denote $F_s(q, t_\infty)$ and $L_3(t_\infty)$ that decayed completely. The white circles denote $F_s(q, t_\infty)$ and $L_3(t_\infty)$ that decayed partially. The color bar indicates the value of $\alpha_2(t^*)$. $\alpha_2^{T,R}(t^*)$ for ϕ 's in between experimental data points were obtained from linear interpolation. Note the break in ϕ axis at $\phi \approx 0.53$. ϕ_g^T and ϕ_g^R , obtained from MCT scaling analysis, are shown by squares in (a) and (b), respectively.

and with Δu , while we observed a minimum in $\alpha_2^T(t^*)$ [Fig. 3(a)] at intermediate attraction strengths, we do not see this for $\alpha_2^R(t^*)$ [Fig. 3(b)]. This clearly implies a melting of the glass only in the translational DOF and is consistent with our observations that in contrast to $F_s(q, t_\infty)$ [Figs. 2(a) and 3(a)], $L_n(t_\infty)$ [Figs. 2(b) and 3(b)] shows only a partial decay. Lending further credit to these observations, while the MCT-predicted ϕ_g^T shows systematic reentrant behavior [Fig. 3(a)], within experimental certainty, ϕ_g^R [Fig. 3(b)] does not.

Why do we see a two-step glass transition for intermediate Δu ?—To address this question, we quantified the structure and body frame dynamics of ellipsoids for $\phi \approx \text{RG}\phi_g$ with Δu . The structure was isotropic for $\Delta u = 0$ [Fig. 1(d)]. For $\Delta u = 1.16$, however, depletion enhanced lateral alignment of ellipsoids resulting in quasi-long range ordering [Fig. 4(a)]. This was further evidenced by the absence of the peak in pair correlation function, $g(r)$, [Fig. 4(b)] and a higher value of static orientational correlation function, $g_2(r)$ [33], [Fig. 4(c)] at $\frac{r}{2w} = 1.7$,

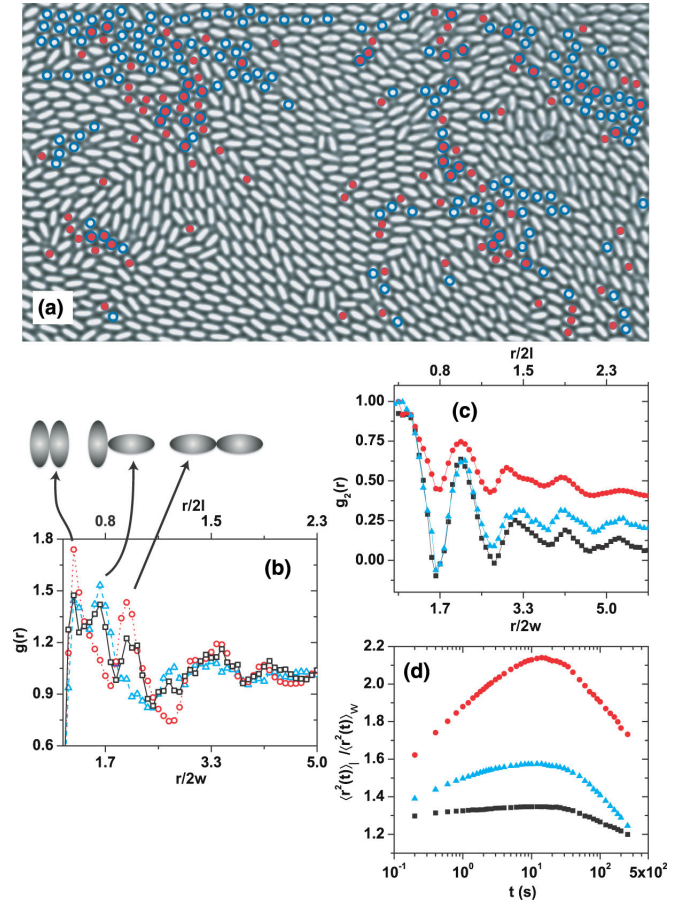


FIG. 4 (color online). (a) Top 10% orientationally (solid) and translationally (hollow) most-mobile particles at $\Delta u = 1.16$ and $\phi = 0.81$. Subfigures (b)–(d) show $\Delta u = 0$ at $\phi = 0.79$ by black squares, $\Delta u = 1.16$ at $\phi = 0.81$ by red circles, and $\Delta u = 1.47$ at $\phi = 0.81$ by cyan triangles. (b) $g(r)$. (c) $g_2(r) = \langle \cos(2[\theta(0) - \theta(r)]) \rangle$. (d) Ratio of mean-squared displacements along major and minor axis of ellipsoids.

corresponding to perpendicular alignment of ellipsoids. At higher Δu 's, the longer bond-life time precluded the ellipsoids from sampling various configurations and led to small domain sizes (Supplemental Material, movie 2 [19]). Consistent with the above observations, we find that diffusivity along the long axis of ellipsoids is significantly enhanced as compared to their short axis at $\Delta u = 1.16$ [Fig. 4(d)]. Thus, while interparticle attractions free up volume and shift ϕ_g^T to a higher $\phi = 0.84 \pm 0.01$, quasi-long-range ordering hinders rotational relaxation and results only in a marginal shift in $\phi_g^R = 0.82 \pm 0.01$. Further, we find that the orientationally most-mobile particles are predominantly at interdomain boundaries and the translationally most-mobile particles are in the ordered regions [Fig. 4(a)] [9].

To conclude, our experiments highlight for the first time, the crucial role of particle shape and interaction anisotropy in reentrant glass phenomena. We have shown that 2D suspensions of colloidal ellipsoids ($\alpha = 2.1$) with purely

repulsive interactions show a single glass transition. This is in qualitative agreement with MMCT predictions in 3D [13]. Owing to the lack of pseudonematic ordering, we find that an appreciable fraction of orientationally most-mobile particles are also translationally most-mobile. Confirming theoretical predictions [29], we found that MCT scaling laws can be readily extended to systems with short-range attraction as well. Interestingly, quasi-long-range ordering is promoted at intermediate Δu 's and results in a two-step glass transition with an intervening orientational glass regime. Although our experiments showed clear reentrant behavior only in the translational DOF, it would be worthwhile to investigate the role of α on reentrant glass dynamics. Further, it would be of immense interest to quantify dynamics in the vicinity of the A_3 singularity [6,29] in glasses of ellipsoids. We expect our results to stimulate further experiments, theory and simulations.

C.K.M. thanks Hima Nagamanasa and Shreyas Gokhale for useful discussions. R.G. thanks ICMS, JNCASR for financial support.

*To whom all correspondence should be addressed.
chandank@jncasr.ac.in

†To whom all correspondence should be addressed.
rajeshg@jncasr.ac.in

- [1] C. A. Angell, *Science* **267**, 1924 (1995); F. H. Stillinger, *ibid.* **267**, 1935 (1995).
- [2] P. N. Pusey and W. van Megan, *Nature (London)* **320**, 340 (1986).
- [3] W. K. Kegel and A. van Blaaderen, *Science* **287**, 290 (2000).
- [4] E. R. Weeks, J. C. Crocker, A. C. Levitt, A. Schofield, and D. A. Weitz, *Science* **287**, 627 (2000).
- [5] K. N. Pham, A. M. Puertas, J. Bergenholtz, S. U. Egelhaaf, A. Moussaid, P. N. Pusey, A. B. Schofield, M. E. Cates, M. Fuchs, and W. C. K. Poon, *Science* **296**, 104 (2002); T. Eckert and E. Bartsch, *Phys. Rev. Lett.* **89**, 125701 (2002).
- [6] K. Dawson, G. Foffi, M. Fuchs, W. Götze, F. Sciortino, M. Sperl, P. Tartaglia, Th. Voigtmann, and E. Zaccarelli, *Phys. Rev. E* **63**, 011401 (2000).
- [7] S. Torquato and F. H. Stillinger, *Rev. Mod. Phys.* **82**, 2633 (2010) and references therein.
- [8] R. C. Kramb, R. Zhang, K. S. Schweizer, and C. F. Zukoski, *Phys. Rev. Lett.* **105**, 055702 (2010).
- [9] Z. Zheng, F. Wang, and Y. Han, *Phys. Rev. Lett.* **107**, 065702 (2011).
- [10] H. Cang, J. Li, V. N. Novikov, and M. D. Fayer, *J. Chem. Phys.* **119**, 10421 (2003).
- [11] C. De Michele, R. Schilling, and F. Sciortino, *Phys. Rev. Lett.* **98**, 265702 (2007).
- [12] P. Pfeiderer, K. Milinkovic, and T. Schilling, *Europhys. Lett.* **84**, 16003 (2008).
- [13] M. Letz, R. Schilling, and A. Latz, *Phys. Rev. E* **62**, 5173 (2000).
- [14] Q. Chen, S. C. Bae, and S. Granick, *Nature (London)* **469**, 381 (2011); D. J. Kraft, R. Ni, F. Smallenburg, M. Hermes, K. Yoon, D. A. Weitz, A. van Blaaderen, J. Groenewold, M. Dijkstra, and W. K. Kegel, *Proc. Natl. Acad. Sci. U.S.A.* **109**, 10787 (2012).
- [15] K. A. Dawson, *Curr. Opin. Colloid Interface Sci.* **7**, 218 (2002).
- [16] A. Latka, Y. Han, A. M. Alsayed, A. B. Schofield, A. G. Yodh, and P. Habdas, *Europhys. Lett.* **86**, 58001 (2009); L. J. Kaufman and D. A. Weitz, *J. Chem. Phys.* **125**, 074716 (2006); N. B. Simeonova, R. Dullens, D. Aarts, V. de Villeneuve, H. Lekkerkerker, and W. Kegel, *Phys. Rev. E* **73**, 041401 (2006).
- [17] S. Asakura and F. Oosawa, *J. Chem. Phys.* **22**, 1255 (1954); S. Kruger, H. J. Mogel, M. Wahab, and P. Schiller, *Langmuir* **27**, 646 (2011).
- [18] C. C. Ho, A. Keller, J. A. Odell, and R. H. Ottewill, *Colloid Polym. Sci.* **271**, 469 (1993).
- [19] See Supplemental Material at <http://link.aps.org/supplemental/10.1103/PhysRevLett.110.188301> for ensuring quasi-2D nature of cell, $F_s(q, t)$ and $L_5(t)$, MSD and $P(\Delta r(t^*))$ for purely repulsive system, quantification of Δu from dimer lifetime measurements, and determination of ϕ_0 .
- [20] J. C. Crocker and D. G. Grier, *J. Colloid Interface Sci.* **179**, 298 (1996); see standard software (MATLAB codes) at <http://people.umass.edu/kilfoil/downloads.html>.
- [21] W. Kob and H. C. Andersen, *Phys. Rev. Lett.* **73**, 1376 (1994).
- [22] W. Gotze and L. Sjogren, *Rep. Prog. Phys.* **55**, 241 (1992); W. Gotze, *J. Phys. Condens. Matter* **2**, 8485 (1990).
- [23] T. Shen, C. Schreck, B. Chakraborty, D. E. Freed, and C. S. O'Hern, *Phys. Rev. E* **86**, 041303 (2012).
- [24] G. Adam and J. H. Gibbs, *J. Chem. Phys.* **43**, 139 (1965).
- [25] Y. Han, A. M. Alsayed, J. Zhang, T. C. Lubensky, and A. G. Yodh, *Science* **314**, 626 (2006).
- [26] T. Narumi, S. V. Franklin, K. W. Desmond, M. Tokuyama, and E. R. Weeks, *Soft Matter* **7**, 1472 (2011).
- [27] S. C. Glotzer, *J. Non-Cryst. Solids* **274**, 342 (2000).
- [28] C. Donati, S. C. Glotzer, P. H. Poole, W. Kob, and S. J. Plimpton, *Phys. Rev. E* **60**, 3107 (1999).
- [29] K. A. Dawson, G. Foffi, F. Sciortino, P. Tartaglia, and E. Zaccarelli, *J. Phys. Condens. Matter* **13**, 9113 (2001); A. M. Puertas, M. Fuchs, and M. E. Cates, *Phys. Rev. Lett.* **88**, 098301 (2002).
- [30] E. Zaccarelli and W. C. K. Poon, *Proc. Natl. Acad. Sci. U.S.A.* **106**, 15203 (2009).
- [31] A. Sheu and S. A. Rice, *Phys. Rev. E* **72**, 011407 (2005).
- [32] J. R. Savage, D. W. Blair, A. J. Levine, R. A. Guyer, and A. D. Dinsmore, *Science* **314**, 795 (2006).
- [33] J. A. Cuesta and D. Frenkel, *Phys. Rev. A* **42**, 2126 (1990).